Superconducting Qubit with Purcell Protection and Tunable Coupling

J. M. Gambetta,[1] A. A. Houck,[2] and Alexandre Blais[3]

[1]*Institute for Quantum Computing and Department of Applied Mathematics, University of Waterloo, Waterloo, Ontario, Canada N2L 3G1*

[2]*Department of Electrical Engineering, Princeton University, Princeton, New Jersey 08544, USA*

[3]*Département de Physique, Université de Sherbrooke, Sherbrooke, Québec, Canada J1K 2R1*

(Received 21 September 2010; published 20 January 2011)

We present a superconducting qubit for the circuit quantum electrodynamics architecture that has a tunable qubit-resonator coupling strength g. This coupling can be tuned from zero to values that are comparable with other superconducting qubits. At $g = 0$, the qubit is in a decoherence-free subspace with respect to spontaneous emission induced by the Purcell effect. Furthermore, we show that in this decoherence-free subspace, the state of the qubit can still be measured by either a dispersive shift on the resonance frequency of the resonator or by a cycling-type measurement.

DOI: 10.1103/PhysRevLett.106.030502 PACS numbers: 03.67.Lx, 03.65.Yz, 42.50.Pq, 85.25.Cp

Decoherence is one of the major problems facing quantum information processing. To overcome this problem the theories of quantum error correction [1] and decoherence-free subspaces (DFS) [2] have been developed. A DFS is a subspace of a system which exploits symmetries in the decoherence process to allow the system to be completely decoupled from the environment. As an example, the spontaneous decay of a multilevel atom to a common bath can be cancelled by quantum interference for a particular state [3].

In parallel, superconducting qubits have emerged as strong candidates for quantum information processing [4]. These are systems which are designed using Josephson junctions to make low loss nonlinear oscillators. They are designed so that two levels (qubit) can be isolated, controlled, and measured, properties which are usually mutually exclusive. With *sweet-spot* operations [5–7] and material engineering [8], there has been tremendous progress. This is evidenced by the recent demonstration of two qubit quantum algorithms [9], high fidelity single qubit gates [10], high fidelity two [11,12] and three [13,14] qubit entangled states, and Bell violation [15].

Currently the most successful superconducting qubits are the flux [6], phase [8], and transmon [7], as these qubits are essentially immune to offset charge (charge noise) by design. The transmon receives its charge noise immunity by operating at a point in parameter space where the energy level variation with offset charge, the charge dispersion, is exponentially suppressed. This suppression has experimentally been observed and results in this qubit being approximately T_1 limited ($T_2 \approx 2T_1$) in the circuit quantum electrodynamics (QED) architecture [16]. In this architecture, illustrated in Fig. 1(a), the qubits are coupled to a coplanar waveguide resonator through a Jaynes-Cummings Hamiltonian operated in the dispersive regime [17]. This resonator acts as the channel to control, couple, and readout the state of the qubit.

In circuit QED, an important mechanism for T_1 has been shown to be Purcell decay [18]. This is a fundamental relaxation that arises when a qubit is coupled to a resonator. It can be understood as dressing of the qubit by the resonator field; the dressed qubit contains a photonic part whose amplitude is proportional to the coupling strength g divided by the detuning Δ between the qubit and resonator. This photonic component relaxes at a rate given by the resonator decay rate κ. As a result, the dressed qubit relaxes at a rate $\gamma_1^{\mathrm{Pur}} = \kappa g^2/\Delta^2$. To overcome the Purcell decay, one can either work at large detunings, use a Purcell filter [19], or design a Purcell protected qubit.

In this Letter we present a three island device that acts as a qubit (two levels, arbitrary control, and measurement) and has the ability to *independently* tune both the transition frequency and coupling strength g while still exhibiting exponential insensitivity to charge noise and maintaining an anharmonicity equivalent to that of the transmon and phase qubit. This tunable coupling qubit (TCQ), illustrated in Fig. 1(b), can be tuned from a configuration where it is

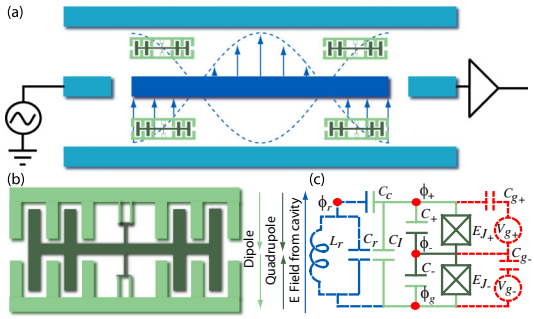

FIG. 1 (color online). (a) Schematic of the circuit QED architecture. (b) Schematic of the proposed three island device. The islands are connected by SQUIDs and the arrows are used to indicated the dipole and quadrupole moments of the device. (c) Circuit model of the device. The variables are explained in the text.

totally Purcell protected from the resonator $g = 0$ (in a DFS) to a configuration which couples strongly to the resonator, with values comparable to those realized for the transmon. Furthermore, we show that in the DFS a strong measurement can be performed. The TCQ only needs to be moved from the DFS configuration for single and two-qubit gates [20]. In the off position, all multiqubit coupling rates are therefore zero. That is, in the circuit QED architecture [see Fig. 1(a)] the TCQ-resonator coupling could be used to induce a tunable coupling between non-nearest neighbor TCQs [17]. This adds to the previous approaches which use external circuit elements as tunable couplers [21–23].

As illustrated in Fig. 1(b), the essential idea behind the TCQ is a three island version of the transmon. This device, like the transmon, has a dipole moment between each island. These dipoles can add in parallel, resulting in a larger dipole moment, or in an antiparallel configuration, creating a quadrupole moment. This device therefore supports two modes, with only the dipole moment coupling to the resonator. That is, the mode corresponding to the quadrupole moment is a DFS with respect to Purcell decay and can be used for storing quantum information. Because of the capacitance between the top and lower island C_I, these modes couple. The ratio of quadrupole to dipole moment can be tuned by changing the energy of the upper and lower islands.

The reduced circuit model representing this device is shown in Fig. 1(c). The solid green lines represent the components associated with the TCQ, with light green indicating the upper "+" and lower island "−" and the dark green representing the center island. Each island is connected by a Josephson junction of energy $E_{J_\pm}$ and capacitance $C_\pm$ which is taken to include the Josephson capacitance. The resonator is approximated by a parallel LC circuit (blue dashed lines) with inductance L_r and capacitance C_r. C_c represents the capacitive interaction between the TCQ and the resonator. Finally, the dotted red lines represent charge noise resulting from voltage fluctuations $V_{g_\pm}$ that occur inside the device ($C_{g_\pm}$ represent the capacitor coupling for these fluctuations). A similar system was presented in Ref. [24] for the observation of giant nonlinear Kerr effects in circuit QED.

The Hamiltonian of the TCQ is obtained following Ref. [25] with the 3 degrees of freedom being the phase across the junctions $\gamma_+ = (\phi_+ - \phi_-)/\Phi_0$, $\gamma_- = 2\pi\phi_-/\Phi_0$, and the flux across the resonator ϕ_r. Here $\Phi_0 = h/2e$ is the flux quantum and $\phi_\pm$ are the node fluxes defined in Fig. 1(c). We find $H = H_T + H_I + H_R$, where $H_R = \hbar\omega_r a^\dagger a$ is the Hamiltonian of the resonator with $\omega_r = 1/\sqrt{L_r C_r'}$ and a the annihilation operator. H_T is the Hamiltonian for the TCQ and is given by

$$H_T = \sum_\pm 4E_{C_\pm}(n_\pm - n'_{g_\pm})^2 - \sum_\pm E_{J_\pm}\cos(\gamma_\pm) + 4E_I n_+ n_-, \tag{1}$$

with charging energy $E_{C_\pm} = e^2/2C'_\pm$, interaction energy $E_I = e^2/C'_I$, and dimensionless gate voltage $n'_{g_\pm} = n_{g_\pm} + n_{g_\mp}C'_\mp/C'_I$, where $n_{g_\pm} = C_{g_\pm}V_{g_\pm}/2e$. The primes above the capacitances indicate renormalization by the electrostatic interactions. Finally, the TCQ-resonator interaction is represented by the Hamiltonian H_I

$$H_I = 2e^2 V_{\rm rms}(\beta_+ n_+ + \beta_- n_-)(-ia^\dagger + ia), \tag{2}$$

where $\beta_\pm = C_c C_{\Sigma_\mp}/[C_{\Sigma_+}C_{\Sigma_-} + (C_I + C_c)(C_{\Sigma_+} + C_{\Sigma_-})]$, with $C_{\Sigma_\pm} = C_\pm + C_{g_\pm} + C_c$, and $V_{\rm rms} = \sqrt{\hbar\omega_r/2C'_r}$. In the limit where the TCQ is isolated ($C_c = 0$) and symmetric (dropping all $\pm$ in capacitors), then $E_{C_+} = E_{C_-} = E_C$ with $E_C = e^2(C_I + C_\Sigma)/2(C_\Sigma^2 + 2C_I C_\Sigma)$ and $E_I = -2E_C C_I/(C_I + C_\Sigma)$. E_I can be tuned from zero to $-2E_C$ by modifying C_I, which is governed by the direct capacitance between the upper and lower island. This can be made much larger than the interaction energy between two superconducting qubits that are coupled virtually by a resonator [17]. The eigenenergies of the TCQ Hamiltonian are shown in Fig. 2(a) (solid lines) as a function of E_I/E_C for $E_{J_\pm} = 50E_C$. The system has a "V-like" structure with two levels in the first excited manifold and three in the next. As E_I is increased, the degeneracies in the manifolds are lifted and the TCQ becomes a multilevel atom with nonladderlike structure.

In the limit of large $E_{J_\pm}/E_{C_\pm}$, the phases $\gamma_\pm$ are restricted to be around zero and we expand the cosines in H_T to fourth order [7]. As a result, we can model the system as two coupled anharmonic oscillators with the Hamiltonian $H_{T_{\rm eff}} = H_+ + H_- + H_c$, where $H_\pm = \hbar[\omega_\pm + \delta_\pm(b_\pm^\dagger b_\pm - 1)/2]b_\pm^\dagger b_\pm$ and $H_c = \hbar J(b_+ b_-^\dagger + b_+^\dagger b_-)$, with $\omega_\pm = \sqrt{8E_{J_\pm}E_{C_\pm}}/\hbar - E_{C_\pm}/\hbar$, $\delta_\pm = -E_{C_\pm}/\hbar$, and $J = E_I(E_{J_+}E_{J_-}/E_{C_+}E_{C_-})^{1/4}/\sqrt{2}\hbar$. This Hamiltonian can be approximately diagonalized, with small parameter $\delta_\pm/(\tilde\omega_+ - \tilde\omega_-)$, using the transformation $D = \exp[\lambda(b_+ b_-^\dagger - b_+^\dagger b_-)]$ with $\lambda = \tan^{-1}(2J/\zeta)/2 + \theta$ and $\zeta = \omega_+ - \omega_- - (\delta_+ - \delta_-)/2$. Here, $\theta = \pi/2$ for $\zeta < 0$ and $\theta = \pi$ for $\zeta > 0$. Doing this we find

$$\tilde H_{T_{\rm eff}} = \hbar\sum_\pm\left[\tilde\omega_\pm + \frac{\tilde\delta_\pm}{2}(\tilde b_\pm^\dagger \tilde b_\pm - 1)\right]\tilde b_\pm^\dagger \tilde b_\pm + \tilde\delta_c \tilde b_+^\dagger \tilde b_+ \tilde b_-^\dagger b_-, \tag{3}$$

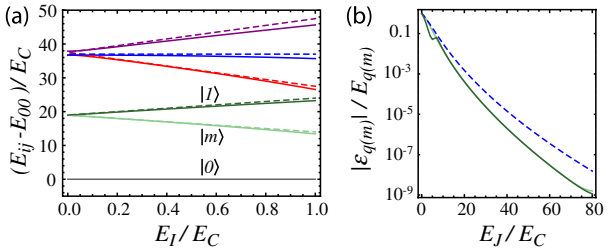

FIG. 2 (color online). (a) Eigenenergies of the TCQ Hamiltonian as a function of E_I/E_C for $E_{J_\pm} = 50E_C$. Solid lines are from numerical diagonalization and dashed lines are from the coupled anharmonic oscillator model. (b) Charge dispersion $|\varepsilon_{q(m)}|$ as a function of the ratio E_J/E_C for $E_I = -E_C$ (solid lines) and $E_I = 0$ (dashed lines).

where $\tilde{\omega}_\pm = \omega_\pm + (\tilde{\delta}_\pm - \delta_\pm)/2 + (\delta_+ + \delta_-)J^2/2\mu^2 \pm \mu/2 \mp \zeta/2$, $\tilde{\delta}_\pm = (\delta_+ + \delta_-)(1 + \zeta^2/\mu^2)/4 \pm \zeta(\delta_+ - \delta_-)/2\mu$, and $\tilde{\delta}_c = 2J^2(\delta_+ + \delta_-)/\mu^2$, with $\mu = \sqrt{4J^2 + \zeta^2}$ and the tilde indicating the diagonalized frame. The coupling has induced a conditional anharmonicity $\tilde{\delta}_c$. It is this anharmonicity that makes this system different from two coupled qubits as it ensures that $E_{11} \neq E_{01} + E_{10}$. The superscript ij refers to i excitations in the dark mode ("+") and j excitations in the bright mode ("−"). The choice of these names will be made clear below. The dotted lines in Fig. 2(a) are the predictions from this effective model, which agree well with the full numerics. Thus, from the effective model, the anharmonicities are all around E_C when $|J| > |\zeta|$. The TCQ has not lost any anharmonicity in comparison to the transmon or phase qubit, and, with simple pulse shaping techniques, arbitrary control of the lowest three levels is possible [26]. In terms of the bare states, the qubit is formed by the space $\{|0\rangle = |00\rangle, |1\rangle = |\tilde{10}\rangle = (|10\rangle - |01\rangle)/\sqrt{2}\}$, and $|m\rangle = |\tilde{01}\rangle = (|10\rangle + |01\rangle)/\sqrt{2}$ is used for qubit measurement (see below).

With charge fluctuations being a leading sources of noise in superconducting circuits, we must ensure that quantum information in the TCQ is not destroyed by charge noise. Following Ref. [7], the dephasing time T_ϕ for the qubit (q) and level m will scale as $1/|\varepsilon_{q(m)}|$, where $\varepsilon_{q(m)}$ is the peak-to-peak value for the charge dispersion of the qubit $(0-1)$ and measurement $(0-m)$ transition, respectively. The dispersion in the energy levels arises from the gate charges n'_{g_α} and the fact the potential is periodic. Since the coupled anharmonic oscillator model does not capture the full Josephson potential, charge dispersion is investigated numerically. We expect, as the transmon, this will exponentially decrease with E_J/E_C, as in this limit the effects of tunneling from one minima to the next becomes exponentially suppressed. This is confirmed in Fig. 2(b) which shows $|\varepsilon_{q(m)}|/E_{q(m)}$ (the numerical maximum and minimum of the energy level over n'_{g_α}) as a function of E_J/E_C for $E_I = E_C$ and $E_I = 0$ (transmon limit). Here $E_{q(m)}$ is the qubit (measurement) energy. This confirms that the TCQ has the same charge noise immunity as the transmon.

We now investigate how the two modes of the TCQ couple to the resonator. We start by using the anharmonic oscillator model with the rotating-wave approximation on Eq. (2). Doing this we find $\tilde{H}_{I_{\text{eff}}} = \hbar\sum_\pm \tilde{g}_\pm(a\tilde{b}^\dagger_\pm + a^\dagger\tilde{b}_\pm)$, where $\tilde{g}_\pm = g_\pm\cos(\lambda) \pm g_\mp\sin(\lambda)$ and $g_\pm = \sqrt{2}e^2\beta_\pm V_{\text{rms}}(E_{J_\pm}/8E_{C_\pm})^{1/4}/\hbar$. One of these coupling strengths can be set to zero for an appropriately chosen λ, or maximized to a value similar to that of a transmon. For J negative, it is $\tilde{g}_+$ which can be set to zero; hence, the choice of name "dark" for the "+" state and "bright" for the "−" state. We have numerically confirmed that this model approximately predicts the matrix elements of the charge operators found in H_I, and hence the coupling rates, for the first three manifolds (six levels). Using these six levels we can use perturbation theory to find an effective description of the situation where both the bright and dark modes of the TCQ have a dispersive interaction with the resonator, $|\Delta_\pm| \gg |\tilde{g}_\pm|$ with $\Delta_\pm = \tilde{\omega}_\pm - \omega_r$. To second order in $\tilde{g}_\pm/\Delta_\pm$, we find that the resonator-TCQ interaction induces both a Lamb shift on the TCQ and a TCQ state dependent pull on the resonator. The qubit $(0-1)$ transition frequency becomes $\omega_q = \tilde{\omega}_+ + \tilde{g}_+^2/\Delta_+$ and the $0-m$ transition frequency becomes $\omega_m = \tilde{\omega}_- + \tilde{g}_-^2/\Delta_-$. For states $k = 0, 1, m$ the resonator frequency is $\omega_r + \chi_k$ with resonator pull $\chi_0 = -\tilde{g}_-^2/\Delta_- - \tilde{g}_+^2/\Delta_+$, $\chi_1 = (\tilde{\delta}_+ - \Delta_+)\tilde{g}_+^2/\Delta_+(\tilde{\delta}_+ + \Delta_+) - \tilde{g}_-^2/(\tilde{\delta}_c + \Delta_-)$, and $\chi_m = (\tilde{\delta}_- - \Delta_-)\tilde{g}_-^2/\Delta_-(\tilde{\delta}_- + \Delta_-) - \tilde{g}_+^2/(\tilde{\delta}_c + \Delta_+)$. All states $|0\rangle$, $|1\rangle$, and $|m\rangle$ correspond to different resonator frequencies and can thus be measured by probing transmission of the resonator.

Purcell decay can be evaluated using the same perturbation theory by evaluating $\gamma_1^{\text{Pur}} = \kappa|\langle\bar{1}|a|\bar{0}\rangle|^2$, where the bar indicates first order correction to the TCQ levels from the resonator-TCQ interaction. This yields $\gamma_1^{\text{Pur}} = \kappa\tilde{g}_+^2/\Delta_+^2$. Thus, by setting $\tilde{g}_+$ to zero the Purcell effect is canceled to second order. However, the difference between the resonator pull for the $|0\rangle$ and $|1\rangle$ state is nonzero and given by $\chi = \tilde{\delta}_c\tilde{g}_-^2/\Delta_-(\Delta_- + \tilde{\delta}_c)$. This has the same functional form as for the transmon (when $|J| > |\zeta|$) and is detectable with current microwave electronics. Furthermore, signal-to-noise (SNR) arguments from Ref. [27] carry over to this system and we find $\text{SNR} = 4n\eta\chi T_m$. Here, η is the efficiency of collecting photons emitted by the resonator, n is the number of photons in the resonator which should not exceed $n_{\text{crit}} = \Delta_-^2/4\tilde{g}_-^2$ [27], and T_m is the measurement time. Taking realistic values $T_m = 1\ \mu$s, $\chi/2\pi = 10$ MHz, and $\eta = 1/20$ gives a SNR around $13n$. However, much higher values can be obtained by using the following protocol: Set $\omega_m = \omega_r$ and have C_c large enough to ensure that $|\omega_q - \omega_r| \gg |\tilde{g}_\pm|$, then the $0-m$ transition will vacuum Rabi split the cavity transmission if the qubit state is $|0\rangle$, whereas for the qubit state $|1\rangle$ the transmission will be at bare resonator frequency. In this situation, the heterodyne power $\kappa|\langle a\rangle|^2$ in steady state will be $\kappa\xi^2(\tilde{g}_-^2 + \kappa^2/16)/(\tilde{g}_-^2 + \kappa^2/16 + \xi^2)^2$ [28] for $|0\rangle$ and $4\xi^2/\kappa$ for $|1\rangle$ with ξ the cavity drive amplitude at drive frequency ω_r. Taking $\text{SNR} = \eta T_m\kappa(|\langle a\rangle_0|^2 - |\langle a\rangle_1|^2)$, we find values as large as 1000 for $\tilde{g}_-/2\pi = 100$ MHz, $\kappa/2\pi = 10$ MHz, and $\xi = \tilde{g}_-$. This is similar to a cycling-type measurement and is quantum nondemolition (after wait time κ). In practice, there will be limitations on size of ξ due to the finite anharmonicity of the TCQ.

To achieve tuning of $\tilde{g}_+$ we modify the original circuit and replace the Josephson junctions by SQUIDs with Josephson energy $E_{J_\pm}^{(1)}$ and $E_{J_\pm}^{(2)}$ [see Fig. 1(b)]. The only change in the above theory is the replacement $E_{J_\pm} \rightarrow E_{J_\pm}^{\max}\cos(\pi\Phi_{x_\pm}/\Phi_0)\sqrt{1 + d^2\tan^2(\pi\Phi_x/\Phi_0)}$, with $E_{J_\pm}^{\max} = E_{J_\pm}^{(1)} + E_{J_\pm}^{(2)}$, $d = (E_{J_\pm}^{(1)} - E_{J_\pm}^{(2)})/E_{J_\pm}^{\max}$, and $\Phi_{x_\pm}$ is the external flux applied to each SQUID which we assume to be independent (this is not required but simplifies the

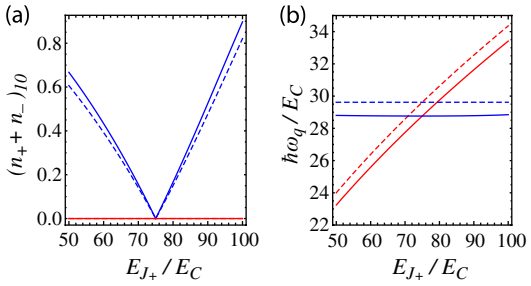

FIG. 3 (color online). (a) Matrix element for the coupling operator $(n_+ + n_-)$ and (b) the qubit transition energy as a function of the energy ratio E_{J_+}/E_C. Other parameters are $n_{g_\pm} = 0$, $E_I = -E_C$, and E_{J_-} is numerically solved to ensure that only the coupling strength [dark (blue)] and frequency [light (red)] are changed. Solid lines are from a numerical diagonalization and dashed lines are from the coupled anharmonic oscillator model.

discussion). This independent control makes it possible to change $E_{J_\pm}$ independently, which in turn allows independent control on $\tilde{g}_+$ and ω_q. To illustrate this we consider the symmetric case and plot in Fig. 3 the normalized coupling strength $\tilde{g}_+\hbar/2e^2V_{\rm rms}\beta$ [3(a)] and $\tilde{\omega}_q$ [3(b)] as a function of the ratio E_{J_+}/E_C. Here, $E_I = -E_C$ and E_{J_-} is numerically solved to ensure that only the coupling rate [dark (blue)] and frequency [light (red)] vary, respectively, for both the full numerical (solid) and effective model (dashed). In the full numerical model, we use $\tilde{g}_+ = 2e^2V_{\rm rms}\langle 1|(\beta_+ n_+ + \beta_- n_-)|0\rangle/\hbar$. The independent control is clearly observed. While the numerical investigation presented here is restricted to the symmetric case, independent tunable $\tilde{g}_+$ (from zero to large values) and ω_q still occurs for nonsymmetric devices.

With this extra control channel there is the possibility of additional qubit decoherence from flux fluctuations. An estimate for flux induced relaxation is $\gamma_1^{\rm flux} = \sum_\pm |\langle 0|\partial H/\partial\Phi_{x_\pm}|1\rangle|^2 M_\pm^2 S_{I_\pm}(\omega_q)/\hbar^2$, where $M_\pm$ is the mutual inductance between the bias line and the TCQ, and $S_{I_\pm}(\omega_q)$ is the spectrum of current noise in the bias line which takes the form $S_{I_\pm}(\omega_q) \approx \hbar\omega_q/R$ at low temperatures [29]. Taking $M = 200\Phi_0/A$, $R = 50\Omega$, $E_{J_\pm}^{\rm max}/h = 20$ GHz, $E_C/h = E_I/h = 0.35$ GHz, and $d = 10\%$, we find $T_1 \approx 1$ s. To estimate dephasing we assume $1/f$ noise and use $T_\phi \approx |\partial\omega_q/\partial\Phi_{x_\pm}|^{-1}/A_\phi$ [30], where A_ϕ is the flux noise at 1 Hz which, for similar superconducting devices, has been measured to be $10^{-6}\Phi_0/\sqrt{\rm Hz}$ [31]. This yields $T_\phi \approx 20$ μs at $\Phi_{x_\pm} = \pi\Phi_0/4$. These values are consistent with the T_1 and T_ϕ predictions for the transmon from flux noise [7]. The additional flux lines thus give independent control of both the coupling and transition frequency while not adding any extra noise with respect to the transmon.

In conclusion we have presented a new device for quantum information processing with superconducting circuits. It is an extension of the transmon and uses quantum interference to achieve independent control of both the qubit-resonator coupling strength and transition frequency. Furthermore, it can be tuned to a decoherence-free subspace with respect to relaxation induced by the Purcell effect, while still allowing efficient readout of its quantum state. It also offers the possibility of implementing a cycling-type measurement.

We acknowledge D. I. Schuster, L. S. Bishop, and R. J. Schoelkopf for valuable discussions. J. M. G. was supported by CIFAR, Industry Canada, MITACS, MRI, and NSERC, A. A. H. by the Alfred P. Sloan Foundation and the David and Lucile Packard Foundation, and A. B. by NSERC, the Alfred P. Sloan Foundation, and CIFAR.

[1] E. Knill and R. Laflamme, Phys. Rev. A **55**, 900 (1997).
[2] D. A. Lidar, I. L. Chuang, and K. B. Whaley, Phys. Rev. Lett. **81**, 2594 (1998).
[3] S.-Y. Zhu and M. O. Scully, Phys. Rev. Lett. **76**, 388 (1996).
[4] R. J. Schoelkopf and S. M. Girvin, Nature (London) **451**, 664 (2008).
[5] D. Vion *et al.*, Science **296**, 886 (2002).
[6] T. P. Orlando *et al.*, Phys. Rev. B **60**, 15 398 (1999).
[7] J. Koch *et al.*, Phys. Rev. A **76**, 042319 (2007).
[8] J. M. Martinis *et al.*, Phys. Rev. Lett. **95**, 210503 (2005).
[9] L. DiCarlo *et al.*, Nature (London) **460**, 240 (2009).
[10] J. M. Chow *et al.*, Phys. Rev. A **82**, 040305(R) (2010).
[11] M. Steffen *et al.*, Science **313**, 1423 (2006).
[12] J. M. Chow *et al.*, Phys. Rev. A **81**, 062325 (2010).
[13] L. DiCarlo *et al.*, Nature (London) **467**, 574 (2010).
[14] M. Neeley *et al.*, Nature (London) **467**, 570 (2010).
[15] M. Ansmann *et al.*, Nature (London) **461**, 504 (2009).
[16] J. A. Schreier *et al.*, Phys. Rev. B **77**, 180502 (2008).
[17] A. Blais *et al.*, Phys. Rev. A **75**, 032329 (2007).
[18] A. A. Houck *et al.*, Phys. Rev. Lett. **101**, 080502 (2008).
[19] M. D. Reed *et al.*, Appl. Phys. Lett. **96**, 203110 (2010).
[20] Note that with external flux lines this is not needed.
[21] T. Hime *et al.*, Science **314**, 1427 (2006).
[22] M. S. Allman *et al.*, Phys. Rev. Lett. **104**, 177004 (2010).
[23] R. C. Bialczak *et al.*, arXiv:1007.2219 [Phys. Rev. Lett. (to be published)].
[24] S. Rebic, J. Twamley, and G. J. Milburn, Phys. Rev. Lett. **103**, 150503 (2009).
[25] M. H. Devoret, in *Quantum Fluctuations*, edited by S. Reynaud, E. Giacobino, and J. Zinn-Justin (Elsevier, New York, 1997).
[26] F. Motzoi *et al.*, Phys. Rev. Lett. **103**, 110501 (2009).
[27] J. Gambetta *et al.*, Phys. Rev. A **77**, 012112 (2008).
[28] L. S. Bishop *et al.*, Nature Phys. **5**, 105 (2009).
[29] R. J. Schoelkopf *et al.*, in *Noise and Information in Nanoelectronics, Sensors, and Standards*, edited by L. B. Kish *et al.*, SPIE Proceedings Vol. 5115 (SPIE, Bellingham, WA, 2003), pp. 356–376.
[30] J. M. Martinis *et al.*, Phys. Rev. B **67**, 094510 (2003).
[31] F. Yoshihara *et al.*, Phys. Rev. Lett. **97**, 167001 (2006).